Proceedings of International Conference on Sustainable Development (ICSD 2019)
In Association with Novateur Publications IJIERT-ISSN No: 2394-3696
ISBN. No. 978-93-87901-05-6
February, 14th and 15th, 2019

ICSD/07

ATTENUATION OF FLOW SEPARATION IN A NACA 8410 TURBINE CASCADE USING GURNEY FLAPS

T. Nilavarasan
Department of Aerospace Engineering, Defence Institute of Advanced Technology, Pune, India
nlvrsnt_phd2015@diat.ac.in

Ganapati N. Joshi
Department of Mechanical Engineering, Defence Institute of Advanced Technology, Pune, India

Sunil Chandel
Department of Mechanical Engineering, Defence Institute of Advanced Technology, Pune, India

Abstract

The effect of Gurney Flaps on a NACA 8410 turbine cascade has been numerically studied. The blade angle of the cascade was maintained at 30º throughout the investigation. The Gurney Flaps were located at the trailing edge of the blades at an angular position of 45º with respect to the chord of the blade. The aerodynamic performance of the cascade at different inflow angles was evaluated with two Gurney Flaps of sizes 1% and 2% of the blade chord length. The results showed that, the Gurney Flaps substantially increased the lift produced by the turbine blades by altering the pressure distributions on both the suction and pressure side of the blade. The skin friction distributions on the suction side of the blades depicted a significant delay in the onset of flow separation due to the presence of the Gurney Flap. They also induced a significant increase in the exit Mach number and the flow turning angle under all the inflow angles that were studied.

Keywords: Turbine cascade, Flow separation, Flow Control, Gurney Flap, Lift Augmentation, Aerodynamic Efficiency

1. Introduction

The aerodynamic performance characteristics of axial turbine and axial compressor cascades play a vital role in the design and development of Gas Turbine Engines. The flowfields around these cascades are highly complex in nature due to the presence of various flow phenomena like unsteadiness, transition, flow separation etc. These flow characteristics greatly affect the efficiency and performance of the compressor or the turbine. Therefore the flow through cascades need to be thoroughly studied in order to understand the flow physics and to manipulate or modify the flowfield to improve the overall performance of the system.

The air flow through highly loaded blades of compressors and turbines tend to separate from the blade surfaces at off design conditions. Flow separation results in a reduction of Lift and hence more number of blades may be required to produce the desired turning. Flow control techniques and devices energize the boundary layer that grows over the turbine or compressor blades through active or passive methods to evade or delay the separation of the fluid from the surface. This improves the Lift force produced by a single blade, which in turn results in lesser number of blades being required to produce the same turning. This directly translates to a decline in the total weight of the compressor or turbine which is particularly advantageous in aircraft applications.

Different active and passive flow control techniques have been elaborately studied for rotordynamics and turbomachinery applications over the last few decades (Bons et.al (2001), Culley et.al (2003), Evans et.al (2008), Reijnen (1997), Chima (2002), Gammerdinger (1995)). One such technique is providing small tabs at the trailing edge of the blades called Gurney Flaps. These Gurney Flaps are small projections, usually located in the trailing edge of airfoils that enhances the lift produced by altering the pressure distributions around the airfoil (Liebeck (1978), Neuhart and Pendergraft (1988), Storms and Jang (1994)). Giguere et.al (1997) noted that, the

optimum height of the Gurney Flap scales with the boundary layer thickness at the trailing edge and usually ranges from 1% to 2% of the airfoil chord length. Studies by Brown and Filippone (2003), have also dictated semi-empirical relations between the height of the Gurney Flap, the free stream velocity and the chord length. One study conducted by Myose et.al (2006) on Compressor Cascades equipped with Gurney Flap reported delay in the onset of stall conditions. Recent numerical investigations by Nilavarasan et.al (2018) showed that Gurney Flaps significantly increased the aerodynamic efficiency of the blades in the cascade at lower inflow angles and substantially improved the performance under post stall conditions.

This paper describes the effect of Gurney Flaps on a NACA 8410 turbine cascade. The Gurney Flaps of height 1% and 2% of the chord length were investigated for their ability to enhance the lift generated. They were located at the trailing edge of the blades at an angular position of 45° with the blade chord. The cascades were investigated at a Mach number of M = 0.2 at different inflow angles. The skin friction distribution over the blades were also analysed to study the flow separation characteristics. The flow structures at the vicinity of the gurney flap that affect the aerodynamic performance of the cascade were also analysed.

2. Computational methodology

2.1. The Governing Equations

The commercial CFD code, STARCCM+ has been used for the computations. The finite volume based code discretizes the integral, steady and compressible Navier Stokes equations that are solved are given below,

$$\int_A \rho \vec{V}.d\vec{a} = 0 \qquad (1)$$

$$\int_A (\rho \vec{V}.d\vec{a})\vec{V} + \int_A P d\vec{a} - \int_A \vec{T}.d\vec{a} = 0 \qquad (2)$$

$$\int_A \rho H \vec{V}.d\vec{a} + \int_A P\vec{V} d\vec{a} - \int_A (\vec{T}.d\vec{a})\vec{V} = 0 \qquad (3)$$

where, $\vec{T}$ is the Viscous Stress Tensor and *P, ρ,* $\vec{V}$ and *H* and are Pressure, Density, Velocity and Total enthalpy per unit mass respectively.

A density based, coupled implicit, Algebraic Multi-Grid (AMG) solver was employed, which used the Gauss Seidal Relaxation Scheme. The discretization of the flow parameters is second order accurate in space. The Dynamic Viscosity is computed through the Sutherland Law. The Reynolds Stresses were modelled by applying the one equation turbulence model developed by Spalart and Allmaras (1992). The only transport equation of the Spalart Allmaras turbulence model is given below:

$$\frac{d}{dt}\int_V \rho\bar{\nu}\, dV + \int_A \rho\bar{\nu}\,(\mathrm{v} - \mathrm{v}_g).da = \frac{1}{\sigma_{\bar{\nu}}}\int_A (\mu + \rho\bar{\nu})\nabla\bar{\nu}.da + \int_V [C_{b2}\,\rho(\nabla\bar{\nu}.\nabla\bar{\nu}) + G_{\bar{\nu}} - \gamma_{\bar{\nu}} + S_{\bar{\nu}}]dV \qquad (4)$$

where, $G_{\bar{\nu}}, \gamma_{\bar{\nu}}$ and $S_{\bar{\nu}}$ are the Production, Dissipation and the user specified Source term respectively.

The turbulent viscosity (μ_T) is calculated from the transport variable as shown below:

$$\mu_T = \rho\bar{\nu}\, F_{\nu 1} \qquad (5)$$

where,

$$F_{\nu 1} = \frac{\chi^3}{\chi^3 + C_{\nu 1}} \qquad (6)$$

and,

$$\chi = \frac{\bar{\nu}}{\nu} \qquad (7)$$

The empirical constants in the equation, viz. $\sigma_{\bar{\nu}}$, C_{B2} and C_{v1} are equal to 0.667, 0.622 and 7.1 respectively.

2.2. Cascade and Gurney Flap Geometry

The schematic diagram of the turbine cascade configuration under study is shown in Fig 1(a). The cascade geometry has been chosen from the experimental studies conducted by Schlichting [15] The cascade has NACA 8410 blades arranged together with unit solidity (D/C = 1) at a blade angle (β_B) of 30°. The inflow angle of the blade (β_i) is the summation of the blade angle (β_B) and the Angle of Attack (α).

$$\beta_i = \alpha + \beta_B \qquad (8)$$

Fig 1(b) depicts the Gurney Flap which is a small protrusion from the trailing edge of the blade. Gurney Flaps of lengths (L), 1% and 2% of the blade chord length have been investigated in this study for their effects on the aerodynamic performance of the turbine cascades. Throughout this study, the Gurney Flaps are positioned at 45° to the blade chord as

shown in Fig 1(b). Also, the thickness (t) of the Gurney Flaps is maintained as 0.33% of the blade chord length.

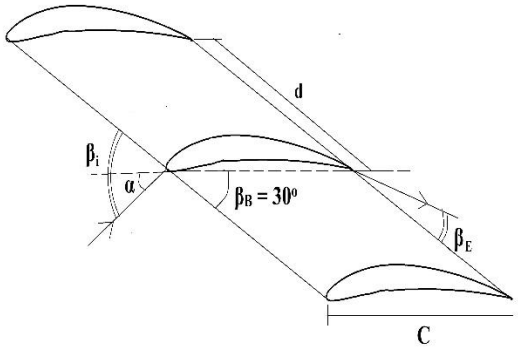

Fig 1 (a). Schematic representation of the turbine cascade under study

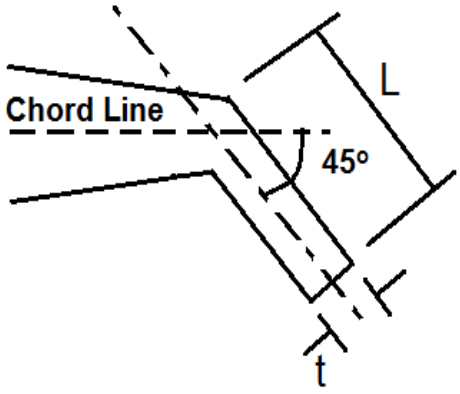

Fig 1 (b). Dimensions, Location and Angular Position of the Gurney Flap

2.3. Computational domain

The Computational domain displayed Fig 2, is a two-dimensional rectangular box that surrounds 5 blades arranged in a cascade. The domain extends up to 5 times the chord length ahead of the leading edge of the middle blade and 10 times the chord length behind the trailing edge of the middle blade in the direction parallel to the blade chord. In the direction normal to the chord, the domain extends to 1.5 times the chord length from the chord of the middle blade on either directions.

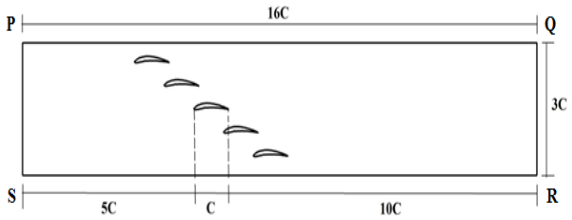

Fig 2. Computational Domain

2.4. Grid Generation

A uniform grid was generated throughout the computational domain, which consisted of quadrilateral cells. The regions close to the blade surfaces were provided with prism layer grids to accurately compute the velocity gradients in the boundary layer. The prism layer is resolved up to the wall which yields a minimum cell wall distance of y^+_{min} = 1.3 in the direction normal to the walls. A greater mesh density is provided in proximity to the Gurney Flaps in order to ensure that their effects on the flowfield are properly accounted for (Fig 3).

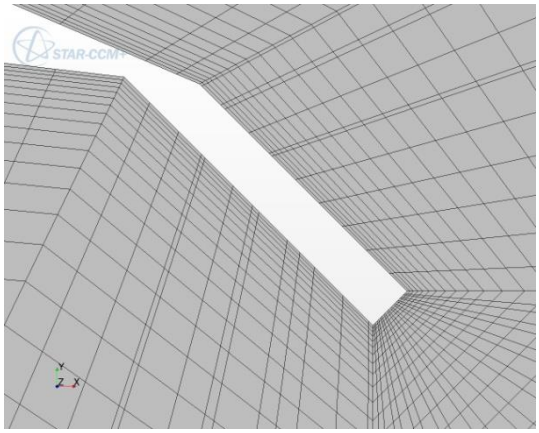

Fig 3. Mesh Refinement close to the Gurney Flap

Grid Independence studies were conducted on the plain bladed configuration with three grids of varying densities (with 43062, 110460 and 242564 number of cells) to determine the optimum grid density required for the computations. It was found that, the grid density corresponding to the grid with 110460 cells was the optimum one, as increasing the grid density beyond that only yielded a maximum deviation of 1.5% in the aerodynamic force characteristics. The number of cells corresponding to all the three configurations are tabulated in Table 1.

Table 1. Number of Grid Cells for all three configurations

Configuration	Number of Cells
Plain Blade Cascade	110460
Cascade with 0.01C Gurney Flap	120102
Cascade with 0.02C Gurney Flap	120872

2.5. Boundary Conditions

The boundary conditions for the simulations were also chosen based on the experiments conducted by Schlichting (1957). The boundary PS (Fig 2) is the

Freestream inlet from where a inflow corresponding to a Mach number of M = 0.2 is supplied. It was ensured that a Reynolds number value of 5 x 10^5 (based on the chord length) is achieved in order to accurately imitate the experiment. The cascade blades and the Gurney Flaps were assumed to be adiabatic and no slip walls. The boundary QR (Fig 2) was designated as a Pressure Outlet and the sides PQ and RS of the computational domain was set to freestream conditions. In all the simulations, the inflow air was assumed to have a turbulent intensity of 10% and a turbulent viscosity ratio of 10. The solution was iterated until the residuals of all the governing equations fell below 1 x 10^{-3}.

2.6. Performance Parameters

The effect of Gurney Flaps on the turbine cascade was studied by comparing the Lift and Drag force coefficients acting on the blades under different inflow angles ranging from 35º to 70º in steps of 5º.

The Lift and Drag force coefficients of the cascade blades are given by,

$$\text{Lift Coefficient, } C_L = \frac{L}{\frac{1}{2}\rho V^2 S} \qquad (9)$$

$$\text{Drag Coefficient, } C_D = \frac{D}{\frac{1}{2}\rho V^2 S} \qquad (10)$$

The change in the Aerodynamic Efficiency due to the Gurney Flaps is also observed at different inflow angles.

$$\text{Aerodynamic Efficiency} = \frac{L}{D} = \frac{C_L}{C_D} \qquad (11)$$

The Lift force produced by the turbine blade is due to the Static pressure and Wall Shear Stress distributions on the surface of the blades. Therefore, the Coefficient of Pressure (C_P) and the Skin Friction Coefficient (C_F) along the blade surface is closely studied to note down the variations in the distribution that attributed to the change in the Lift force generated by the blade. The formulae used for calculating C_P and C_F are given below:

$$C_P = \frac{P - P_1}{P_0 - P_1} = \frac{P - P_1}{\frac{1}{2}\rho V^2} \qquad (12)$$

where, P is the static pressure on the blade surface, P_1 is the static pressure at the freestream and P_0 is the total pressure.

$$C_F = \frac{\tau_w}{\frac{1}{2}\rho V^2} \qquad (13)$$

where, τ_w is the Wall Shear Stress.

2.7. Code Validation

The validation of the computational code and the turbulence model was done by comparing the computationally generated static pressure distributions around the Plain blade with the experimentally measured values provided by Schlichting [15]. The plot comparing the experimental and computational pressure distributions is shown in Fig 4. The plot corresponds to an inflow angle of 50º (AOA = 20º). There is an excellent agreement (maximum deviation of 2%) between the computational and experimental distributions on the pressure side of the blade. On the suction side, a reasonably good agreement is observed throughout, except in the region close to the leading edge of the blade.

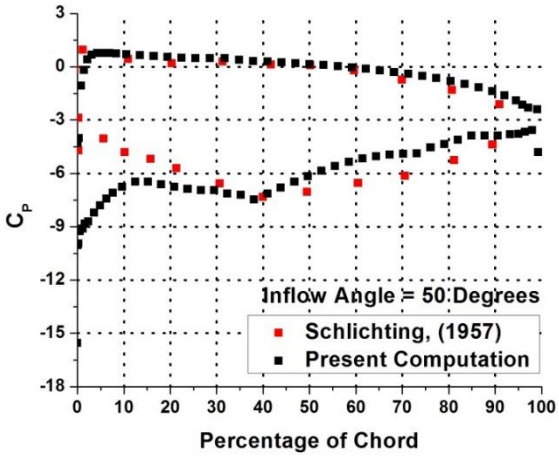

Fig 4. Comparison of Experimental [15] and Computational Pressure Distributions around the Plain Bladed Cascade

3. Results and discussions

3.1. Aerodynamic Performance Characteristics

The placement of Gurney Flaps at the trailing edge of the cascade blades greatly influenced the aerodynamic performance. There was notable variations in the Lift and Drag characteristics of the cascade blades as seen in Fig 5 and 6. As expected, a substantial Lift Augmentation is observed due to the presence of the Gurney Flaps. The Gurney Flap with 0.02C length generated the highest Lift at all the Inflow angles. Although this is a desirable trait, the Gurney Flap also carries a minor Drag penalty and the amount of increment in Drag increases with the Inflow angle as observed from Fig 6. This drag is a form of induced drag as it is a direct by-product of the Lift enhancement. The drag increase is due to the vortical structures present behind the Gurney Flap

which tend to pull the blade along the flow direction due to the low pressure.

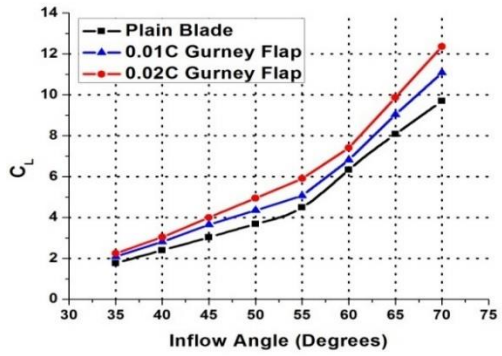

Fig 5. Variation of Lift Coefficient with inflow angle

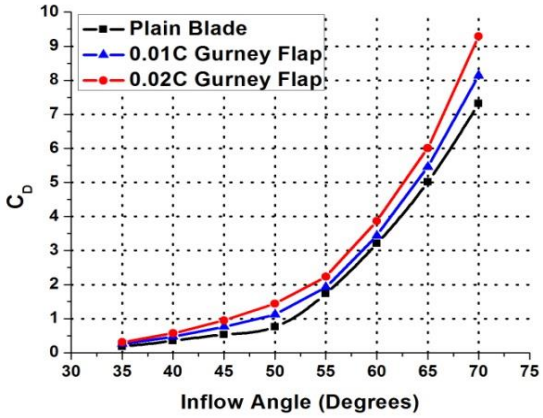

Fig 6. Variation of Drag Coefficient with inflow angle

Because of the above mentioned attributes, there is a small drop in the Aerodynamic Efficiency due to the presence of the Gurney Flap as depicted in Fig 7. As the inflow angle increases, the Aerodynamic Efficiency tends to recover, but remains less than that of the Plain Bladed Configuration.

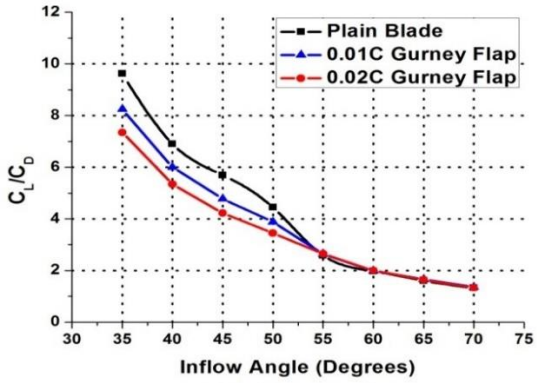

Fig 7. Variation of Aerodynamic Efficiency with inflow angle

3.2. Static Pressure Distributions

The Lift Augmentation in the cascade blades is due to the alteration of the static pressure distributions. The Gurney Flaps tend to obstruct the flow in the pressure side of the blade and turn it over, thereby increasing the static pressure on the surface. On the other hand, the low pressure behind the Gurney Flap produces a low pressure region for the gas in the suction side to rush into. This facilitates a simultaneous drop in the static pressure acting on the suction side of the blade. This effect is clearly visualized in the static pressure distributions plotted in Fig 8 (a-d). This phenomena amplifies the already existing pressure difference between the suction and pressure sides of the blade, enhancing the Lift produced by the blade.

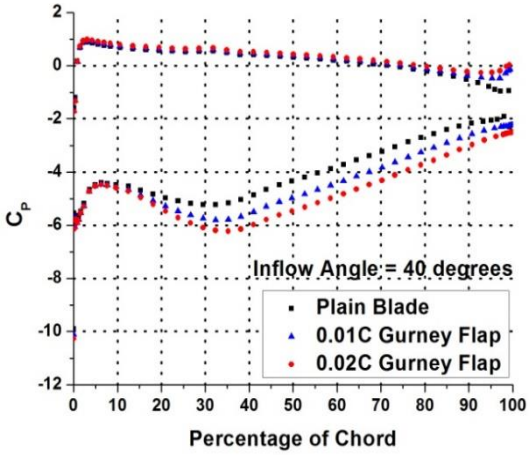

Fig 8 (a). Static Pressure Distributions at $\beta_i = 40^o$

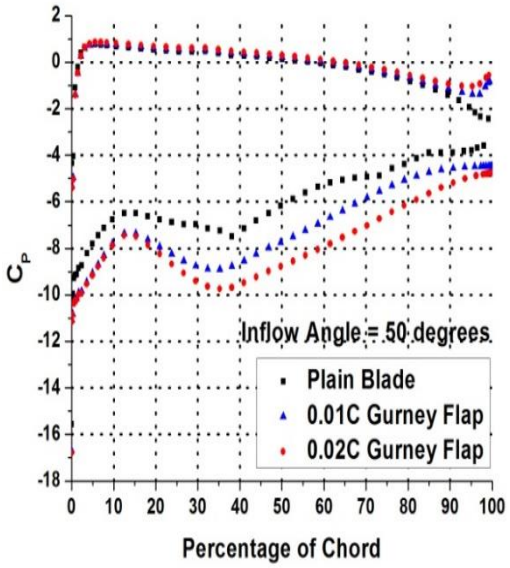

Fig 8 (b). Static Pressure Distributions at $\beta_i = 50^o$

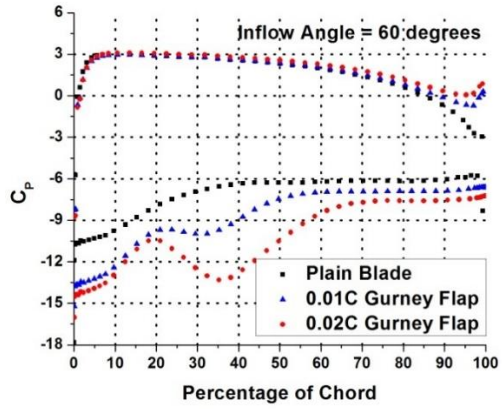

Fig 8 (c). Static Pressure Distributions at β_i = 60º

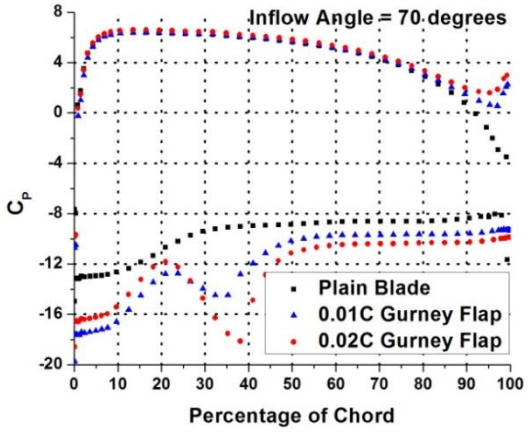

Fig 8 (d). Static Pressure Distributions at β_i = 70º

3.3. Skin Friction Distributions

As the Gurney Flap accelerates the flow on the suction side of the airfoil, the boundary layer on the suction side is also energized. This increase in the momentum of the suction side boundary layer successfully evades flow separation to a larger extent and stays attached to the blade surface.

The skin friction distributions at different Angles of Attack are shown in Fig 9 (a-d). At β_i = 40º, the Plain Bladed cascade experienced the onset of separation at 90% of the chord which was pushed back to 95% by the 0.01C Gurney Flap while, the 0.02C Flap completely eliminated the separation from the flowfield. Similarly, at β_i = 50º, the Plain Blade experienced separation as early as 59% of the chord which was also successfully delayed by the 0.01C and 0.02C Gurney Flaps to 82% and 91% respectively. The skin friction coefficient at the pressure side of the blades were relatively undisturbed due to the presence of the Gurney Flaps.

At higher inflow angles, (β_i = 60º and β_i = 70º), a negative skin friction coefficient near the leading edge of the blade is evident which signifies the presence of a leading edge separation bubble. Although the Gurney Flaps did little to affect this separation bubble, the separation at the rear portion of the blade due to the adverse pressure gradient has been delayed significantly by them.

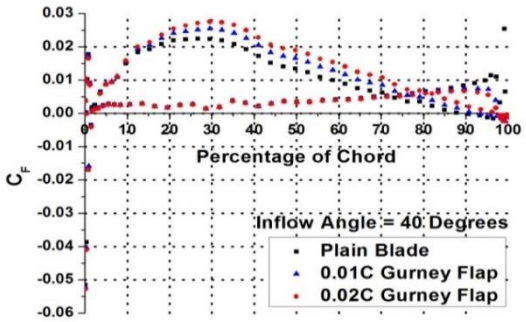

Fig 9 (a). Skin friction Distributions at β_i = 40º

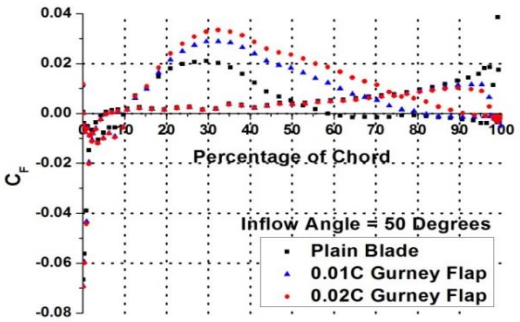

Fig 9 (b). Skin friction Distributions at β_i = 50º

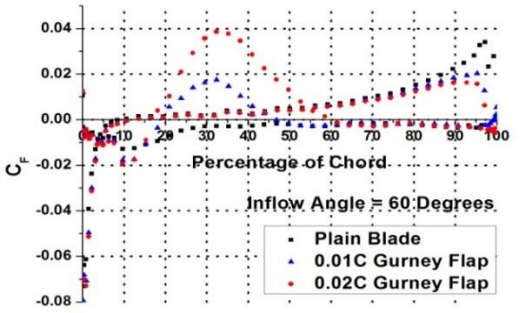

Fig 9 (c). Skin friction Distributions at β_i = 60º

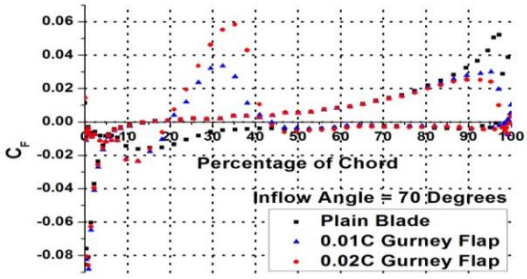

Fig 9 (d). Skin friction Distributions at β_i = 70º

3.4. Vortical Structures

The modifications inflicted by the Gurney Flaps on the aerodynamic characteristics of the turbine cascade are primarily due to the vortical structures induced by them. These structures are formed in the low pressure region behind the Gurney Flap. Fig 10 (a-d) depicts the streamline visualization of these vortical structures formed behind the Gurney Flap with L = 0.02C. In a previous study by Nilavarasan et.al (2018), the Gurney Flaps installed on a cascade with a Blade angle $\beta_B = 90^o$, clearly showed the formation of counter rotating vortex pairs behind the Gurney Flaps. But in the present study, only a single vortex structure is observed at the vicinity of the Gurney Flap. Hence, elaborate experimental and numerical studies need to be carried out to understand the effects of the Blade angle on these vortical structures that are so vital for the effectiveness of the Gurney Flap.

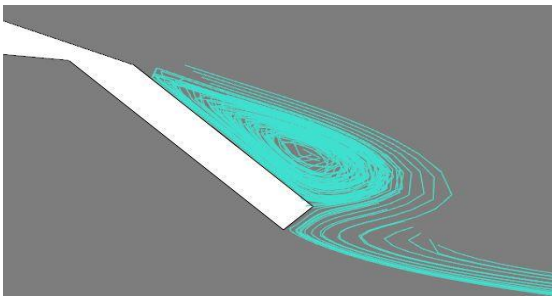

Fig 10 (a). Vortex behind the Gurney Flap at β_i = 40º

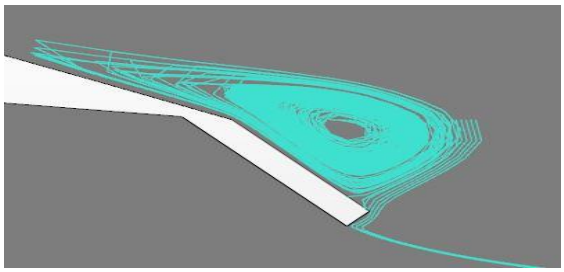

Fig 10 (b). Vortex behind the Gurney Flap at β_i = 50º

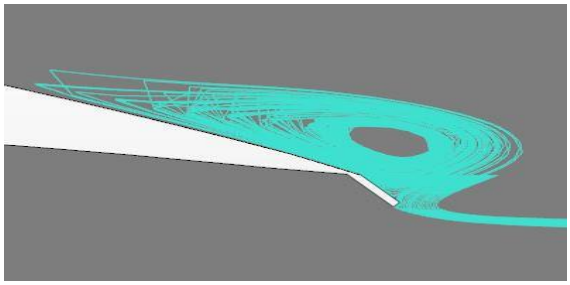

Fig 10 (c). Vortex behind the Gurney Flap at β_i = 60º

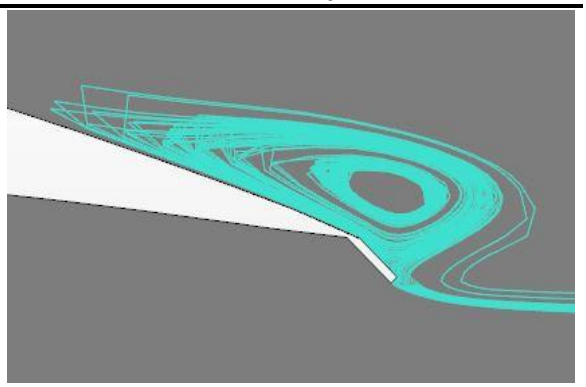

Fig 10 (d). Vortex behind the Gurney Flap at β_i = 70º

3.5. Exit Flow Conditions

The flow Mach number and the angle by which the flow is turned by the blades (β_T) were recorded at the midpoint of the line joining the trailing edges of two consecutive blades. The comparative plots are provided in Fig 11 and 12 respectively. The flow turning angle is calculated by the following equations.

$$\beta_T = \beta_E - \beta_i \qquad (14)$$

where, β_E is the exit flow angle.

$$\beta_E = \tan^{-1} (V_y / V_X) \qquad (15)$$

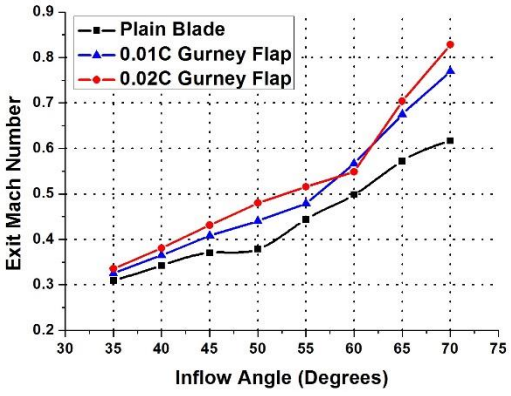

Fig 11. Variation of Exit Mach Number with respect to the Inflow Angle

The exit Mach number was found to increase with increase in the inflow angle. Under all the inflow angles that have been considered, a substantial boost in the exit Mach number was observed in the presence of the Gurney Flaps. Also, the increment was more with the larger Gurney Flap. The flow turning angle initially increased with the inflow angle, but at around $\beta_i = 50^o$, it started to drop. The behavior is attributed to the leading edge separation that is evident from the skin friction distributions.

The Gurney Flaps increased the angle by which the flow turned across the cascade. In both the exit Mach number and the flow turning angle, the best performance was from the cascade with the largest Gurney Flap

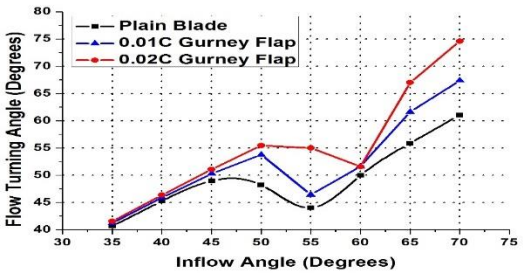

Fig 12. Variation of Flow Turning Angle with respect to the Inflow Angle

4. Conclusion

The effect of Gurney Flaps on the NACA 8410 turbine cascade has been investigated computationally. The cascades with and without Gurney Flaps were subjected to flows at multiple inflow angles and the aerodynamic characteristics have been studied. The following conclusions have been made from the study.

i. The Gurney Flaps significantly enhanced the lift generated by the turbine blades by amplifying the pressure difference between the suction and pressure side of the blades in the cascade.
ii. A small drag penalty was observed due to the presence of the Gurney Flaps due to the vortical stuctures behind the Gurney Flap.
iii. At all inflow angles, a significant increase in the skin friction coefficient is observed at the suction side of the blade due to the presence of the Gurney Flap.
iv. At lower Angle of Attacks, the flow separation on the suction side of the blade due to the adverse pressure gradient was completely eliminated by the 0.02C Gurney Flap.
v. At higher Angle of Attacks, a substantial delay in the onset of separation is observed due to the Gurney Flaps which in turn increases the ability of the blade to produce more Lift and thereby improve the load capacity of the turbine.
vi. A single vortex was observed behind the Gurney Flaps that grew in size with increase in inflow angle.
vii. The exit Mach number and the flow turning angle were higher in the presence of the Gurney Flaps. Their values increased with increase in the size of the Gurney Flaps.

References

1. Bons, J. P., Sondergaard, R., and Rivir, R. B., "Turbine Separation Control Using Pulsed Vortex Generator Jets", *Journal of Turbomachinery*, 123(2), 198–206, 2001.
2. Culley, D. E., Bright, M. M., Prahst, P. S., and Strazisar, A. J., "Active Flow Separation Control of a Stator Vane Using Surface Injection in a Multistage Compressor Experiment", NASA Glenn Research Center TM 2003-212356, 2003.
3. Evans, S.W., Hodson, H. P., Hynes, T. P.,Wakelam, C. T., and Hiller, S. J., "Controlling Separation on a Simulated Compressor Blade Using Vortex Generator Jets", *4th Flow Control Conference, AIAA Paper 2008-4317*, 2008.
4. Reijnen, D. P., "Experimental Study of Boundary Layer Suction in a Transonic Compressor," Ph.D. Thesis, Massachusetts Inst. of Technology, Cambridge, Massachusetts, USA, 1997.
5. Chima R.V., "Computational Modeling of Vortex Generators for Turbomachinery", *ASME Turbo Expo, Paper GT 2002-30677*, 2002.
6. Gammerdinger. P. M., "The effects of Low-Profile Vortex Generators on Flow in a Transonic Fan-Blade Cascade", M.S. Thesis, Naval Postgraduate School, Montenery, California, USA, 1995.
7. Liebeck, R., "Design of Subsonic Airfoils", *Journal of Aircraft*, 15(9), 547-561, 1978.
8. Neuhart, D.H., and Pendergraft, O.C., "A Water Tunnel Study of Gurney Flaps," NASA Technical Memorandum 4071, 1-20, 1988.
9. Storms, B.L., and Jang, C.S., "Lift Enhancement of an Airfoil Using a Gurney Flap and Vortex Generators", *Journal of Aircraft*, 31(3), 542-547, 1994.
10. Giguere, P., Dumas, G., and Lemay, J., "Gurney Flap Scaling for Optimum Lift-to-Drag Ratio", *AIAA Journal*, 35(12), pp. 1888-1890, 1997.
11. Brown, L. and Filippone, A., September "Aerofoil at Low Speeds with Gurney Flaps", *Aeronautical Journal*, 107(1075), 539-546, 2003.
12. Myose. R. Y., Lietsche. J. C., Scholz. D., Zingel. H., Hayashibara. S., Heron. I., "Flow Visualization Study on the Effect of a Gurney Flap in a Low Reynolds Number Compressor Cascade", *AIAA Paper 2006-7809*, 2006.
13. T. Nilavarasan, Ganapati. N. Joshi and Sunil Chandel, "Aerodynamic Performance Characteristics of NACA 0010 cascade with Gurney Flaps", *International Journal of Turbo and Jet Engines*, (Ahead of Print), 2018.
14. Spalart, P. R. and Allmaras, S. R., "A One-Equation Turbulence Model for Aerodynamic Flows" *AIAA Paper 92-0439*, 1992.
15. Schlichting. H., "Cascade Flow Problems", AGARD Report, 93, 1957.